EXPERIMENTAL STUDY OF IMPACT DAMAGE RESISTANCE AND TOLERANCE OF COMPOSITE SANDWICH PANELS

P. Nash, G. Zhou*, S. Gahlay and M. Burt

Department of Aeronautical and Automotive Engineering, Loughborough University, Loughborough, Leicestershire LE11 3TU, UK

* Corresponding author (G.Zhou@Lboro.ac.uk)

Keywords: *unsymmetrical sandwich, impact damage, damage tolerance, CAI strength*

Summary

An experimental study of in-plane compressive behaviour of carbon/epoxy-skinned and E-glass/epoxy-skinned sandwich panels was conducted. For the former, two carbon/epoxy skin thickness combinations were 8/6 plies and 16/12 plies. Both cross ply (CP) and quasi-isotropic (QI) lay-ups were used in each combination. For the latter, two E-glass/epoxy skin thickness combinations of 8/8 and 16/16 plies were used with both being in a cross ply lay-up. The majority of sandwich panels were impact-damaged with their dominant damage mechanisms being characterised. All impact-damaged and baseline panels were in-plane compression tested. The effects of impact damage, lacking symmetry, skin thickness, skin lay-up and core density on CAI strength were examined.

1 Introduction

Composite sandwich structures have been widely used in the aerospace, marine, automotive, railway and wind energy industries because of their high specific bending stiffness and strength against distributed loads. They have increasingly been expected to be damage-tolerant and energy-absorbing under concentrated impact loads. A multitude of damage mechanisms could occur over a range of impact energies, thereby affecting their subsequent residual in-plane compression (popularly known as compression-after-impact (CAI)) performance. When the variation of skin thickness and lay-up, panel symmetry and core density was added, the combined effects on the CAI behavior of the sandwich panels become extremely complex. This has highlighted the need for a thorough understanding of the in-plane compressive behaviour of sandwich structures, in order for these sandwich panels to be effective against localized impacts.

The research programmes at Loughborough University have been carried out to systematically investigate the in-plane compressive behaviour of intact and impact-damaged composite sandwich panels with both aluminium and nomex honeycombs. In two early reports [1-2], damage mechanisms in both aluminium and nomex honeycomb sandwich panels induced via both impact and quasi-static loads were ascertained; the effects of skin thickness, core density and material, indenter nose shape, panel diameter and support condition on the damage characteristics were studied. The energy-absorbing characteristics of the identified damage mechanisms were examined. In a subsequent report [3], the in-plane compressive behaviour of intact and impact-damaged symmetric sandwich panels with aluminium honeycomb core was discussed. This paper presents some results of a further investigation of how the variation of skin thickness and lay-up, panel symmetry and core density affects the in-plane compressive behaviour of composite sandwich panels. The use of the E-glass/epoxy skins were intended to gain the insight of damage propagation in in-plane compression.

2 Sandwich panel manufacture and preparations

Carbon/epoxy laminate skins were made of unidirectional carbon/epoxy 34-700/LTM45 prepreg with a ply thickness of 0.128 mm. For symmetrical panels, both cross-ply lay-up of $(0/90)_{(2)s}$ and quasi-isotropic lay-up of $(45/0/-45/90)_{(2)s}$ were used. For unsymmetrical panels, two combinations of skin thicknesses were used with the same ratio of the thicker skins to the thinner skins. One unsymmetrical panel had a combination of 8 plies and 6 plies in their two skins. The other

unsymmetrical panel had a combination of 16 plies and 12 plies in their two skins. When the lay-up was quasi-isotropic, the thinner skins were in a multi-directional lay-up of $(45/0/-45)_{(2)s}$. Two densities of 5052 aluminium honeycomb core were combined with the carbon/epoxy skins. They were had 70 kg/m^3 and 140kg/m^3 both with a depth of 12.7 mm The denser core was coupled with the thinner cross ply skin arrangement only. Adhesive VTA260 was used for interfacial bonding.

The E-glass/epoxy-skinned sandwich panels were made using the same method as described above. The laminate skins were made of a UD E-glass/epoxy PPG1062/LTM26 prepreg. Two thicknesses of symmetrical E-glass sandwich panels were constructed, a thin 8/8 ply cross ply in $(0/90)_s$, and a thick 16/16 ply cross ply in $(0/90)_{2s}$. As with the carbon/epoxy sandwich panels, a 12.7mm thick 5052 aluminium core with a density of 70kg/m^3 was used with VTA260 adhesive.

Skin laminates of 300×300 mm were laid up and cured in an autoclave at 60°C under a pressure of 0.62 MPa (90 psi) for 18 hours for the carbon/epoxy skins, and 6 hours for the E-glass/epoxy skins. The 0° direction of carbon and glass fibres within the skins was aligned with the ribbon direction of honeycomb core. Each skin was separately bonded to the core in an oven at 60°C for 16 hours under a pressure of 0.1 MPa (15 psi). The sandwich panel was then cut into two nominal 200 mm×150 mm specimens with the longer side aligned with the direction of compressive loading.

After impact, as part of the compression specimen preparation, the core at the panel ends intended for applying compressive load were scored and indented to a depth of about 4 mm (slightly more than one cell size). Epoxy end pots were cast between the two skins to prevent an end-brooming failure and the two potted ends were machined to parallel. Back-to-back strain gauges were then bonded on the panel surfaces at selected locations in both the longitudinal and transverse directions (see Fig. 3(a)) to monitor mean and panel bending strains. These strain data allowed both local and global behaviour of the panels to be examined.

3 Experimental procedures

3.1 Drop-weight impact tests

Impact tests were carried out on an instrumented drop-weight impact rig shown in Fig. 1 by using a hemispherical impactor of 20 mm diameter with a 1.5 kg mass. Impact energies were regulated by selecting desired drop heights and ranged from 5 J to 45 J in this investigation. Each rectangular sandwich panel of 200 mm by 150 mm with a circular testing area of 100 mm in diameter was clamped by using a clamping device. For the unsymmetrical panels, the thicker skin side was impacted. Both impact and rebound velocities were measured respectively and this allows absorbed energies to be calculated directly. Impact force was recorded by a data acquisition system. At some selected impact energy levels, one impacted panel was cut up for an examination of damage mechanisms and the other was compression tested. The range of impact energies for the E-glass/epoxy panels differed slightly to the carbon/epoxy panels, with precaution being taking not to over damage them.

3.2 In-plane compression test

In each in-plane compression test, a panel was placed in a purpose-built support jig, as illustrated in Fig. 3(b). The jig provides simple support along the unloaded edges, which were free to move in the width direction during loading. Quasi-static load was applied to the panel at the machined ends via a Denison testing machine at less than 0.5 mm/ min. Load, strain and cross-head displacement in all tests were recorded. All tested panels were cut up for study of damage mechanisms. The loading direction coincided with the 0^0 direction in the skins of panels.

During the compression tests, a hand held USB microscope, shown in Fig. 2, was set up at the side of the compression jig, giving the ability to capture in-situ sequential images of the central region of the sandwich panels. Pictures were taken at intervals during the test, starting from 15kN, then every 10kN. The intervals were shortened as the expected failure load approached.
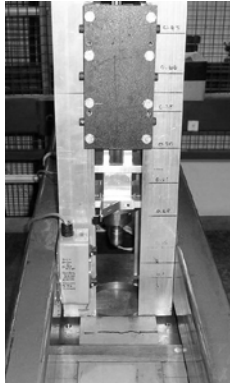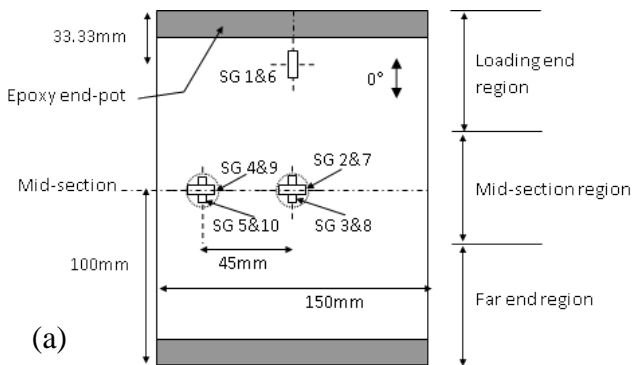
Fig.1. Drop-weight impact test rig

Fig.2. Hand held USB microscope used to capture damage propagation during compression test
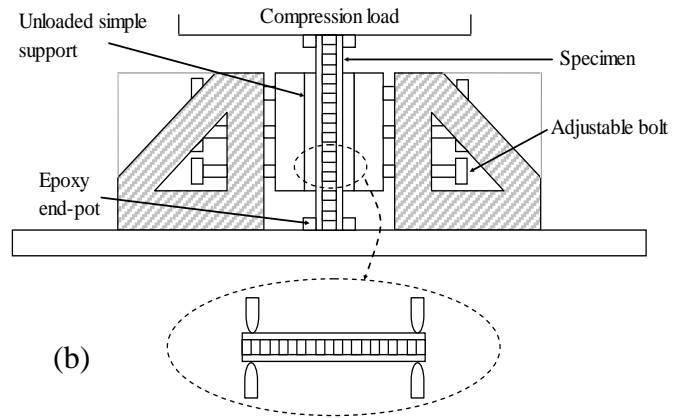

(a)

(b)

Fig.3. (a) In-plane compression specimen and (b) experimental set-up for compression

4 Damage mechanisms and energy absorption

4.1 Thick carbon/epoxy panels with 70kg/m^3 core

The initiation and propagation characteristics of damage mechanisms in impacted sandwich panels in bending were examined extensively via impact response curves, visual observations with the aid of systematic microscopic inspections and cross sectioning. These techniques were shown in [1-3] to be very effective. Thus this approach with the same techniques was deployed for current sandwich panels. Impact at the lower end of the impact energy range typically produces a surface dent, as shown in Fig. 6. A further increase of impact energy resulted in ply fracture on the impacted skin, as shown in Fig. 7.
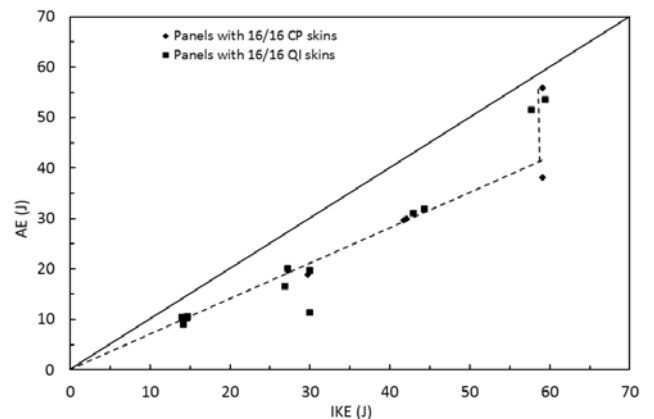

Fig.4. Energy absorption of symmetrical thick panels with 70kg/m^3 core
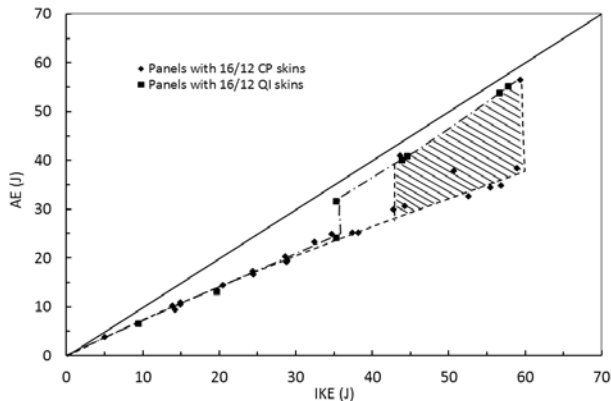
Fig.5. Energy absorption of unsymmetrical thick panels with 70kg/m^3 core

Fig.6. A 16/12 QI carbon/epoxy sandwich panel with 70kg/m^3 core impacted at 35J

Fig.7. A 16/12 QI carbon/epoxy sandwich panel with 70kg/m^3 core impacted at 45J

Current cut–up specimens exhibit the salient features from their damage mechanisms very similar to those established in the symmetrical sandwich panels [1-3]. The initial damage was found to be due to core crushing. In some cases, small delamination in the impacted skin was also observed. The initial damage

was followed by a continued core crushing with either the onset or propagation of delaminations. Eventually, skin ply fracture occurred. These early onset mechanisms are responsible for around 70% of absorbed energy in the panels, for both symmetrical and unsymmetrical panels, as seen in Fig. 4 and Fig. 5, with the occurrence of fiber fracture increasing this absorption to upwards of 95%. In symmetrical panels, the point at which fiber fracture occurs is typically just before 60J (Fig. 4). Comparatively, the unsymmetrical panels exhibit a more ambiguous point of fiber fracture, resulting in a region from 35J up to 60J where fiber fracture has been observed (Fig. 5). A cross section of a damaged unsymmetrical 16/12 panel impacted at 35J is shown in Fig. 8, which shows extensive crushed core and skin delaminations in the impacted (16-ply) skin. The bottom (12-ply) skin remained intact in all cases and the maximum crushed depths at the upper end of the impact energy ranges reached about the middle of cores at the highest impact energy. This offers some experimental evidence to justify the desire for removing a couple of plies in the distal skin for further weight reduction while maintaining the impact damage resistance. There was no local skin-core debonding. The extent of crushed core was generally greater than the extent of skin delamination. There was no noticeable difference in these characteristics between symmetrical and unsymmetrical panels.
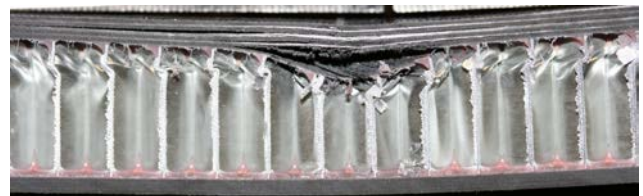

Fig.8. A 16/12 sandwich panel with 70kg/m^3 core impacted at 35J

4.2 Thin carbon/epoxy panels with 70kg/m^3 core

The energy-absorbing characteristics of the impacted thin symmetrical panels are shown in Fig. 9 for two types of panels with skins in cross-ply and quasi-isotropic lay-ups. In the initial region, a linear increase in energy absorption is around two thirds of impact energy. As in the thick panels, the initial damage was found to be due to core crushing, with some delamination observed. The initial damage was

followed by a continued core crushing with either the onset or propagation of delaminations. Once skin fracture occurred, the absorbed energy is increased abruptly up to over 90%. Shown in Fig. 10, the overall energy-absorbing features of unsymmetrical cross-ply and quasi-isotropic panels are very similar to those from the symmetrical panels. It is noticeable that the region in which fiber fracture is likely to occur is once again bigger in the unsymmetrical panels.
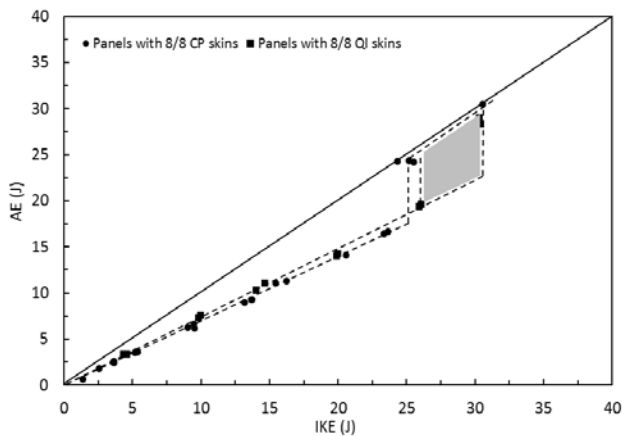

Fig.9. Energy absorption of symmetrical thin sandwich panels with 70kg/m^3 core

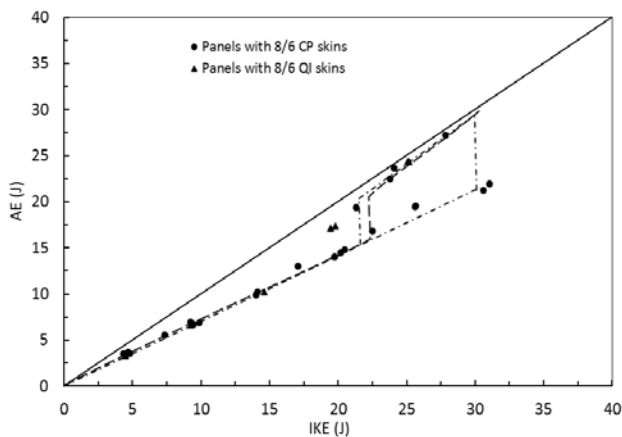Fig.10. Energy absorption of unsymmetrical thin sandwich panels with 70kg/m^3 core

4.3 Thin carbon/epoxy panels with 140kg/m^3 core

Damage mechanisms for the dense core panels differed considerably from the lower density panels. Due to the higher stiffness of the core, initial damage was absorbed by propagation of delamination in the impacted skin, with core crush length being less than the measured delaminations. As the impact energies were increased the development of the delaminations and the core crushing was very limited, considering the continued absorption of the impact energy by the panel with no fiber fracture being noticed, interfacial core/skin debond was occurring in the midrange of the impact energies. Eventually, fiber fracture in the impacted skin was observed, which is coupled with the increase of absorbed energy to above 95%, shown in Fig. 11 as seen in the lower density tests as well. A cross section of a damaged 8/8 panel impacted at 25J is shown in Fig. 12. It is important to note that as in the lower density panels; there is no damage propagation in the distal skin. More importantly, this image shows the contrast between the developments of the damage mechanisms when compared to the lower density core. Immediately it can be seen there is interfacial debonding between the impacted skin and core. Lateral extension of core crush is very limited, and the maximum crushed depth is only just approaching ¼ of the overall core depth. Multiple delaminations in the top skin have extended to extremities of the image. Very few differences in damage propagation and characteristics were noted between symmetrical and unsymmetrical panel arrangements. The only difference of note, seen in Fig. 11, is the earlier onset of fiber fracture in the symmetrical panels. Although the margins are tight, this difference could be due to the slightly higher stiffness of the symmetrical skins, making them more susceptible to localized damage, causing them to be more likely to experience fiber fracture.
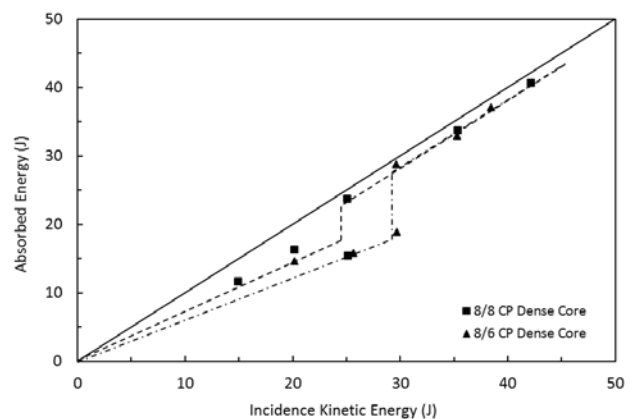
Fig.11 Energy absorption of symmetrical sandwich panels with a core density of 144 kg/m^3

Fig.12. A 8/8 sandwich panel with 140kg/m^3 impacted at 25J

4.4 Symmetrical E-glass/epoxy panels with 70kg/m^3 core

Damage assessment of the impacted E-glass/epoxy panels in comparison to the carbon/epoxy panels due to the translucency of the skins. The 3 usually non visible damage mechanisms can now be identified without the need for destructive inspection. As shown in Fig. 13 by the 3 dashed circles, delamination, debond, and core crush (from inner to outer circles) are all easily recognizable by visual inspection. Interestingly the 0° and 90° directions for core crush and delamination regions can now be recorded, allowing comparison of damage propagation in both main fiber directions.

With the damage mechanisms established, it is identified that in a similar manner seen in the carbon/epoxy panels, initial damage is found to be core crushing, with a sharp increase in core crush length measured in even low impact energies. Due to the similarity in trends in the lower range of impact energies for core crush lengths and absorbed energy, it can be inferred that the core is the primary damage mechanism in initially absorbing the impact, further confirming the importance of the cores role in impact performance as seen in the carbon/epoxy tests. Delaminations were found only in the impacted skin in both thicknesses of panel, with the thick skins developing larger delaminations than then the thin skins at the higher range of the impact energies. This is likely due to energy of the impact being absorbed by the occurrence of interfacial debond in the thin panels between the 10-15J range. Fiber fracture was only observed in the thin skinned panels at 35J, and can be seen in Fig. 15 to increase the energy absorbed to around 95%. The grey region

in the figure indicated an area of uncertainty as to where fiber fracture will definitively occur. As mentioned, a cautious approach was used in testing the thicker panels, with the final impact energies not being enough to cause fracture in the impacted skin, hence the trend is shown to be wholly linear in Fig. 15.

Fig. 16 shows one of only 2 cross sectioned panels used to validate the visual inspections of the damage mechanisms. In the 16 ply panel, which was impacted at 18J, a single delamination at the midpoint of the skin can clearly be seen in the top impacted skin, whereas the bottom skin remains undamaged. Core crush extent can be seen to be the dominating damage mechanism, extending much beyond the delamination length. A small amount of core debond can be seen in the central region under the impact location. Impact at the lower end of the impact energy range typically results in a surface dent in the impacted skin, shown clearly in Fig. 14.

Fig.13. Impact damage in an 8/8 CP E-glass/epoxy panel with 70kg/m^3 core impacted at 15J

Fig.14. Impact damage in an 8/8 CP E-glass/epoxy panel with 70kg/m^3 core impacted at 25J
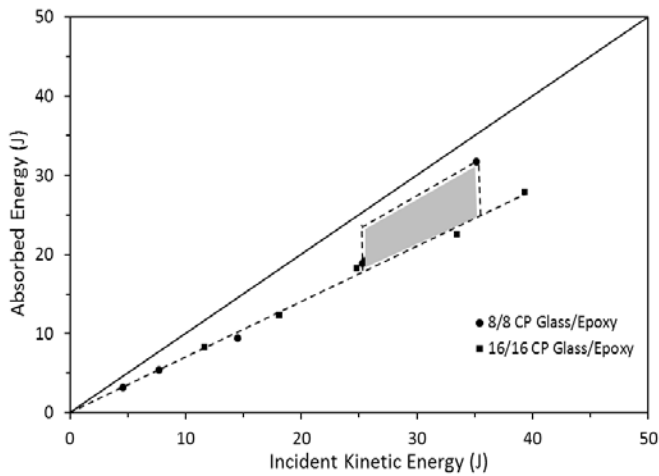
Fig.15. Energy absorption of sandwich panels with E-glass/epoxy skins and with a core density of 70 kg/m^3

Fig.16. A 16/16 E-glass/epoxy sandwich panel impacted at 18J

5 Residual in-plane compressive behaviour

The in-plane residual compressive behaviour of the damaged sandwich panels was very complex due primarily to two factors. One is that the sandwich itself was complex structure on its own during in-plane compression because the two skins were stabilised by the core to some degree. When one skin was impact damaged, the equal contribution from the two identical skins to the compression resistance was lost. The lack of skin symmetry in their construction simply adds a significant additional complexity. Thus, a substantial part of prior knowledge and understanding established from the compression of monolithic panels (e.g. in [4-5]) did not apply. The other is that, while the distal thinner skin remained undamaged after impact, the impacted thicker skin around the mid-section region was damaged with core underneath being crushed. The unequal contribution to the compression resistance initially could be 'evened up' by the

impact damage in the thicker skin. Therefore, the residual compressive performance of the damaged panels was attributed not only to the strength degradation of the compressive skin associated with the damage but also to the lack of symmetry for the panels with respect to the in-plane compression loading and supporting conditions and interaction between the skins and core in each of such panels.

Assessment of the tolerance of the panels starts with the identification of baseline performance. In all constructions put forward in this investigation, trustworthiness of the baseline compressive strength is still suspect due to the complex role the core plays in the compressive resistance. The intact core bonded to undamaged skins throughout provided a stabilising support to the two skins in the TTT direction through normal compression properties and provided a constraint against a relative in-plane compressive movement through TTT shear properties. Thus the relative in-plane compressive movement of the skins in the mid-section region was more restricted than those impact damaged, suggesting that the compressed skins had to shear the core and crush core first or dimple rather than wrinkle outwards. Consequently, the skins that could be equally compressed in the mid-section region had little net shear force to overcome the shear rigidity constraint, thereby shearing the core. With their relatively high flexural rigidity, the intact panels had the significant compressive resistance in the mid-section region. As a result, all the intact panels failed at the location close to one of the panel ends

Nearly all the impact-damaged sandwich panels failed around the mid-section region, which was weakened by the presence of impact damage. An example from the thinner 8/6 panels is shown in Fig. 17, whereas an example from the thicker 16/12 panels is shown in Fig. 18, in which the longitudinal shearing through the core is clearly visible.

Fig.17. Photographs showing a side view of an impact-damaged sandwich panel after CAI test

Fig.18. Photographs showing front and side view of an impact-damaged sandwich panel after CAI test

An example of failed unsymmetrical panels with a dense core is shown in Fig. 19. Unlike the lower density examples above, there is very little evidence of shearing through the core. Looking at the example response for an impacted unsymmetrical panel in Fig. 21 the initial strain response is very linear and steep, differing from the control response in Fig.20 which shows a high level of deformation in the far field location, implying an even application of compressive load in the two skins, helped by the strength of the core constraining the relative in-plane movement of the skins. At approximately 18kN there is clear evidence of damage propagation through the panel, with the most significant deformations in the outer region of the mid-section. Due to the location, the deformation in both longitudinal and transverse directions, and early onset of this event, it is very likely that the skin has debonded from core. Between 20kN and 40kN 2

further incidents cause noticeable increase in strain. An image captured at 40kN shown in Fig. 22 shows a clear propagation of delamination through the mid-section region of the distal thin skin. Since nothing was visible at 35kN, the likely initiation of this is highlighted in Fig. 21. This delamination drastically reduces the resistance in the mid-section, causing failure in this region not long after the delamination propagated. Failure in the mid-section depicted in Fig. 18 is indicative of most mid-section failures, showing arrested skin fracture and kink bands developing in the transverse direction on the impacted side, with severe debond causing bending or compressive failure in the distal skin usually off centre towards the edge of the debonded area.
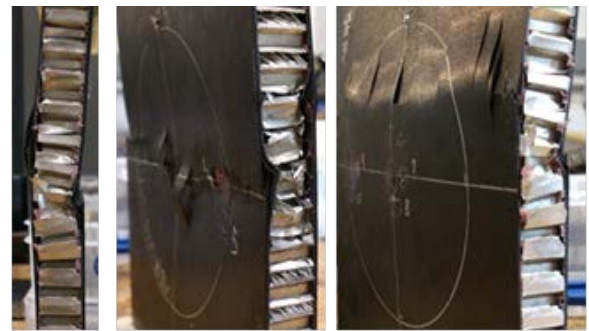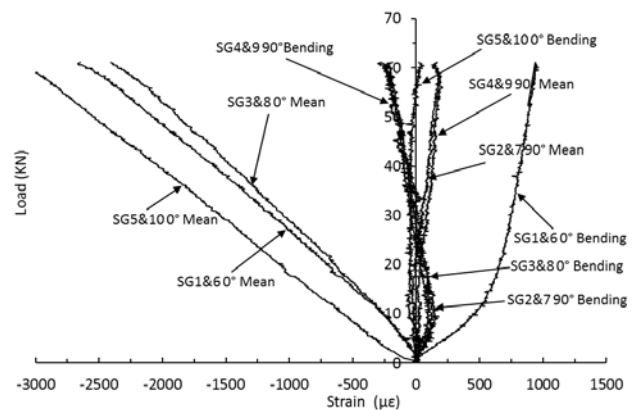

Fig.19. Photographs showing side, front and rear views of impact-damaged 8/6 carbon/epoxy 140kg/m^3 core sandwich panel

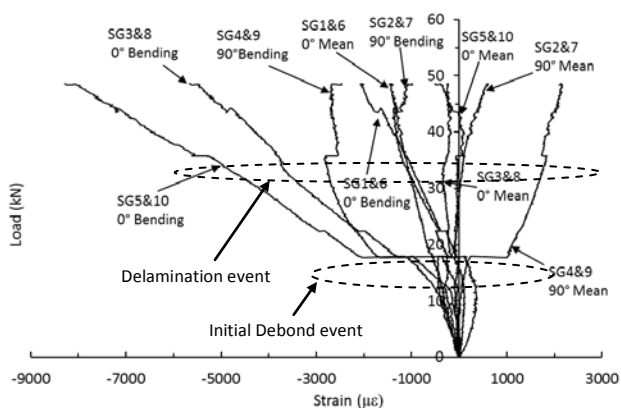Fig.20. Load-strain curves of an in-plane compression test on a 8/6 CP control panel with 140kg/m^3 core

Fig.21. Load-strain curves of an in-plane compression on an 8/6 CP 25J impact-damaged panel with 140kg/m³ core
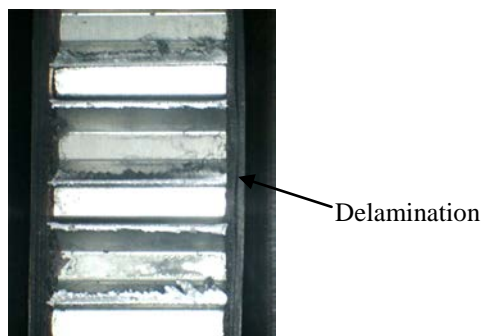

Fig.22. Photograph showing delamination propagation in 8/6 CP carbon/epoxy panel with 140kg/m³ core during test

Similar to the carbon/epoxy panels, establishing an accurate baseline compressive strength proved difficult for this width/length ratio for the E-glass/epoxy panels. Premature end failures were observed in both thin and thick panels. This problem extended into the majority of the thick skinned panels. The toughness of the E-glass construction, as previously mentioned, was underestimated during the impact testing, and the impact range was not sufficient enough to induce mid-section failure in all the thick panels. Hence the compressive data is on the whole fairly untrustworthy. Shown in Fig. 23 is one of the thick panels that failed in the mid-section. Due to the translucency, the failure mechanisms and damage propagation can be seen clearly. Large areas of delamination in the central region would have cause drastic local instabilities in the mid-section region, leading to the failure. The core crush pattern

also shows the sinusoidal mode of bending the panel experienced before failure. Through the thickness fracture is also evident on the impacted skin along the transverse direction.
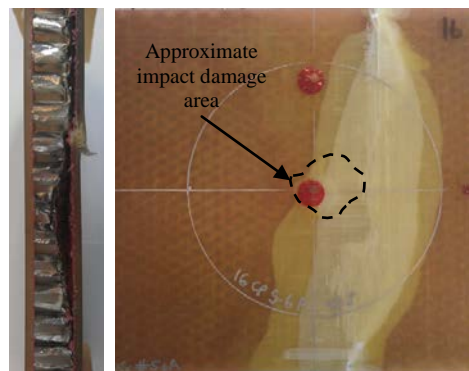

Fig.23. Photographs showing a side and front view of an impacted E-glass/epoxy sandwich panel

The thin impacted E-glass/epoxy panels responded as expected with all impact damaged panels experiencing failure in the mid-section region, with the impact damage, the equal contribution from the two identical skins to the compression resistance was lost, longitudinal shearing of the core was present in all specimens, propagation of debonds and delaminations from the impact caused local instability in the mid-section leading to failure.

6 Impact damage tolerance

6.1 Effect of impact damage

Assessing the effect of impact damage in unsymmetrical sandwich panels in in-plane compression was very difficult, as the lack of symmetry in the sandwich could counteract the effect of impact damage, if the thicker skin is sufficiently damaged. Therefore, a steady reduction trend of CAI strength or strain with an increase of impact energy (IKE) may not be established. This point is clearly shown in Fig. 24 for the thinner unsymmetrical sandwich panels. It is interesting to observe in this figure that these thinner panels were as if very damage-tolerant up to 17 or 18J without suffering any reduction in their CAI strengths. We believe this is because the benefit of two additional plies in the thicker skins was cancelled out by the impact damage such that the baseline values of in-plane compressive strength were as if more or less

unchanged up to about 15J. Around 20 J where ply fracture occurred, CAI strength values have deteriorated further. This implies that the in-plane compressive behaviour of the undamaged unsymmetrical panels may not be as good as those of symmetrical panels. In addition, data from sandwich panels with skins in a lay-up of cross ply seem to show a significant scatter for both baseline and CAI strength values at the lower end of impact energy range. A further examinations of tested panels revealed that the lower strength values were associated with the fact that they failed prematurely at one of the two ends. For the thicker unsymmetrical panels in Fig. 25, a reduction of CAI strength was moderate. Their steady degrading trends are similar to those established for symmetrical sandwich panels in [3]. A further degradation of their CAI strengths after the occurrence of ply fracture is visible but much less obvious. In addition, the effect of lay-up in these thicker unsymmetrical panels on CAI strength is small.
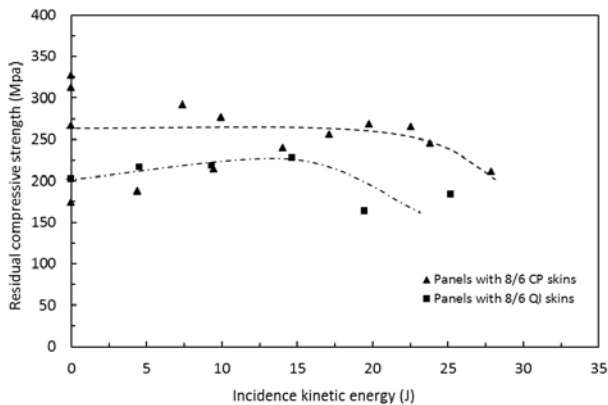

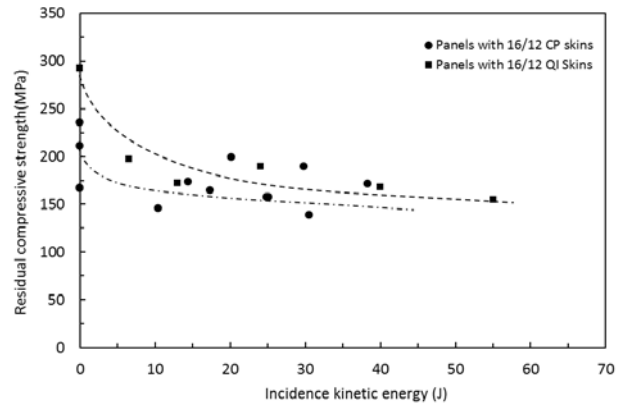Fig.24. A variation of residual compressive strength with IKE for unsymmetrical sandwich panels with 70kg/m^3 core

Fig.25. A variation of residual compressive strength for thick unsymmetrical sandwich panels with 70kg/m^3 core

Damage tolerance for carbon/epoxy panels with a denser core follows the pattern exhibited previously by the lower density examples. The symmetrical panels show a fairly sharp initial drop off in compressive strength, which plateaus in the range of 15-35J, indicating that once the presence of delamination and core crush are established, further increasing these damage mechanisms has little effect on the compressive performance. With the introduction of the fiber fracture mechanism, a further drop off is observed. This trend is almost mirrored by the unsymmetrical panels, the only difference being no initial drop off due to impact damage. The initial compressive strength of the panels is seen to be greater in the symmetrical panels, since the neutral plane no longer coincided with its mid-plane due to its unequal skin thicknesses. However, as previously witnessed, the CAI strength of the unsymmetrical panels experiences a resurgence, due to this initial imbalance being 'evened out' by the thicker skin being subjected to an impact. This can be seen in Fig. 26, with the unsymmetrical panels showing comparative strength to the symmetrical panels up to 30J, with even a hint of improved performance up to this point. The occurrence of fiber fracture in both cases causes a further decrease in compressive resistance.
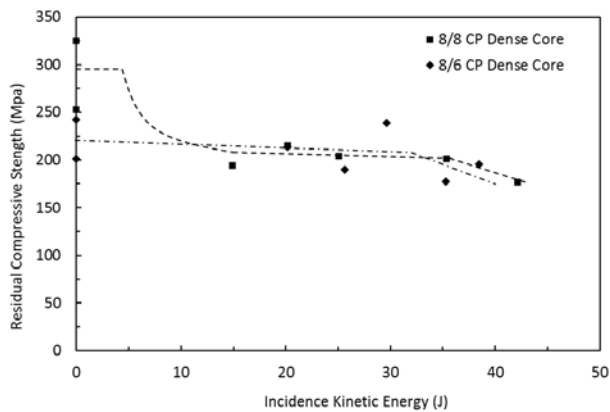
Fig.26. A variation of residual compressive strength with IKE for sandwich panels with 140kg/m^3 core

The damage tolerance, shown in Fig. 27, of the thick 16/16 CP E-glass/epoxy panels is hard to assess at this stage, without obtaining true compressive failures for the impacted panels, the strength values associated with end failure are not accurate. The thin E-glass panels exhibit a fairly good tolerance to impact damage up to around 15J, where a slight drop off in compressive strength is seen as the impact damage is further developed in the panel, with the panel containing a fractured impact skin showing a reduction of around 20%.
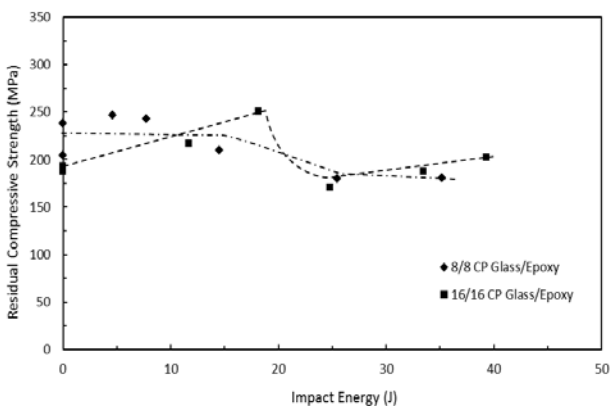

Fig.27. A variation of residual compressive strength with IKE for sandwich panels SG

6.2 Effect of skin thickness

As established in symmetrical carbon/epoxy panel CAI testing, the effect of skin thickness on damage tolerance is small, if not insignificant. Both thick and thin panels in both lay-ups both experience an initial drop below baseline performance after the

occurrence of low energy impacts, following this compressive strength evens out over the midrange of impact energies. Any difference between thicknesses is seen in the tolerance to the occurrence of fiber fracture, with the thicker skinned constructions showing a more muted decay in compressive strength at the higher impact energy levels.

Observing the skin thickness variations in unsymmetrical panels has surfaced one fundamental difference. Thicker skinned unsymmetrical panels behave almost identically to the symmetrical equivalents. However, the thin skins do not experience an initial drop in performance after the application of impact damage. The thin skinned panels are far more sensitive to the uneven compressive loading of skins due to the effective shifting of the neutral plane, leading to the baseline performance suffering compared to the symmetrical counterparts. When the thin unsymmetrical panels undergo impacts, the existing imbalance is effectively evened out, causing a much more symmetrical loading condition, resulting in little or no drop in compressive strength in the lower range of impact energies, as seen in Fig. 24.

For symmetrical E-glass/epoxy panels, it is clear that the toughness of the thicker skinned panels offers a much greater impact resistance than expected, making comparison between the two thicknesses hard to conclude on at this stage.

6.3 Effect of skin lay-up

In thick symmetrical carbon/epoxy panels, and similarly the unsymmetrical counterparts, the notable difference in skin lay-up comes from the base performance for compressive strength. As theory dictates, due to more fibers in the loading direction, CP panels have a higher average compressive strength than QI. However, as trends indicate, seen in Fig. 25 the steepness of the decay in QI panels is shallower than the CP counterparts, implying the QI lay-up offers better damage tolerance.

Thin symmetrical and unsymmetrical panels offer a complex relationship between CP and QI lay-ups. Observing trends in symmetrical panels suggest that the average baseline compressive strength between

lay-ups is very similar, with QI panels having the slightly lower value. Damage tolerance of the QI is however observed to be much superior to the CP constructions. QI panels resist the onset of fiber fracture much more effectively, resulting in no drop off in compressive performance past the point of decay for the CP panels. Effective damage tolerance of impacts over 30J for QI symmetrical panels far out performs the debilitating damage incurred by the CP panels around the 25J mark. Conversely, as seen in Fig. 24, unsymmetrical CP panels consistently perform better than the QI panels, although displaying similar trends.

6.4 Effect of panel symmetry

Panel asymmetry in thick carbon/epoxy constructions has very little effect on compressive performance. Trends from symmetrical and unsymmetrical panels are almost identical, providing very strong evidence that in thicker constructions, the removal of 4 plies from the distal skin could allow for weight saving, without any adverse effects in all round damage resistance and tolerance.

Thin panels offer a slightly more complex relationship based on asymmetry. Whilst unsymmetrical CP constructions offer a slightly lower average baseline performance than the symmetrical equivalents, damage tolerance in the unsymmetrical panels appears to outperform the symmetrical constructions. Conversely, symmetrical QI panels average baseline compressive strength far exceeds that of the unsymmetrical QI panels, and the damage tolerance being far superior in the symmetrical panels. The inclusion of a multi-direction skin in the thin panels clearly results in a significant loss in damage tolerance performance not experience by the thick panel equivalent. As it stands, there is evidence to suggest that weight could be saved by removing plies from the cross ply lay-ups, but it appears that quasi-isotropic thin symmetrical panels offer a clear advantage over the unsymmetrical equivalents.

6.5 Effect of core density

Comparing the symmetrical and unsymmetrical high density core response to the lower density equivalents shows a remarkably similar trend. It is important to note however that the impact range of the higher cores is shifted towards the right hand side of the x-axis. If further impact protection is needed, increasing the core density before first increasing the thickness of the skins in the sandwich construction can offer a lighter weight solution.

The unsymmetrical and symmetrical comparison of the CP dense core panels once again shows that the removal of plies from the distal skin, whilst seeing a drop in baseline performance, damage tolerance is not affected, allowing for the potential in saving further weight from the sandwich constructs.

7 Closing remarks

Unsymmetrical carbon/epoxy composite sandwich panels with core densities of $70kg/m^3$ and $140kg/m^3$ and symmetrical thick and thin E-glass/epoxy sandwich panels were impact-damaged at impact energy ranging from 2 J to 60 J. Both intact and impact-damaged panels were subjected subsequently to in-plane compression. The presence of the core counteracted the deleterious effect of impact damage. While the thicker unsymmetrical panels showed the CAI characteristics similar to symmetrical panels, the thinner panels demonstrated that impact damage in the thicker skin reduced the degree of the effect associated with the lack of symmetry in in-plane compression, thereby enhancing their CAI performance when they were impact-damaged, a characteristic mirrored in the dense core panels. The E-glass/epoxy panels showed encouraging impact absorption qualities, with their translucent properties making damage assessment very accessible without destructive means necessary. The thin panels performed as expected in CAI, with an initial drop off in compressive performance seen due to the loss of equal contribution of the two skins to the compressive load, with further reductions seen with the further development of impact damage mechanisms, culminating in fiber fracture providing the lowest drop off in compressive strength. The thick panels demonstrated extraordinary resistance to lower levels of impact damage, with the panels failing to show true compressive failures even up to 35J.

References

[1] G. Zhou, M.D. Hill and N. Hookham "Damage characteristics of composite honeycomb sandwich panels in bending under quasi-static loading". *J. of Sandwich Structures and Materials*, Vol. 8, pp 55-90, 2006.

[2] G. Zhou, M.D. Hill and N. Hookham "Investigation of parameters governing the damage and energy-absorbing characteristics of honeycomb sandwich panels". *J. of Sandwich Structures and Materials*, Vol. 9, pp 309-342, 2007.

[3] G. Zhou and M.D. Hill "Impact damage and residual compressive strength of honeycomb sandwich panels". *J. of Sandwich Structures and Materials*, Vol. 11, pp 329-356, 2009.

[4] G. Zhou and L. Rivera "Investigation for the reduction of in-plane compressive strength in preconditioned thin composite panels". *Journal of Composite Materials,* Vol. 39, pp 391-422, 2005.

[5] G. Zhou and L. Rivera "Investigation for the reduction of in-plane compressive strength in preconditioned thick composite panels". *Journal of Composite Materials,* Vol. 41, pp 1961-1994, 2007.